
DISCOMAT: Distantly Supervised Composition Extraction from Tables in Material Science Articles

Tanishq Gupta¹, Mohd Zaki², N. M. Anoop Krishnan^{2,3}, Mausam^{3,4}

¹Department of Mathematics, ²Department of Civil Engineering

³Yardi School of Artificial Intelligence, ⁴Department of Computer Science and Engineering
Indian Institute of Technology Delhi

tanishqg2406@gmail.com, {cez198233, krishnan, mausam}@iitd.ac.in

Abstract

A crucial component in the curation of KB for a scientific domain is information extraction from tables in the domain’s published articles – tables carry important information (often numeric), which must be adequately extracted for a comprehensive machine understanding of an article. Existing table extractors assume prior knowledge of table structure and format, which may not be known in scientific tables. We study a specific and challenging table extraction problem: extracting compositions of materials (e.g., glasses, alloys). We first observe that material science researchers organize similar compositions in a wide variety of table styles, necessitating an intelligent model for table understanding and composition extraction. Consequently, we define this novel task as a challenge for the ML community, and create a training dataset comprising 4,408 distantly supervised tables, along with 1,475 manually annotated dev and test tables. We also present DISCOMAT, a strong baseline geared towards this specific task, which combines multiple graph neural networks with several task-specific regular expressions, features, and constraints. We show that DISCOMAT outperforms recent table processing architectures by significant margins.

1 Introduction

Advanced knowledge of a science or engineering domain is typically found in published research papers from that domain. Information extraction (IE) from scientific articles develops ML methods to automatically extract this knowledge for curating large-scale domain-specific KBs (e.g., Ernst et al. [2015], Hope et al. [2021]). These KBs have a variety of uses: they lead to ease of information access by domain researchers Tsatsaronis et al. [2015], Hamon et al. [2017], provide data for development of domain-specific ML models Nadkarni et al. [2021], and potentially help in accelerating scientific discoveries Jain et al. [2013], Venugopal et al. [2021]. Significant research exists on IE from text of research papers (see Nasar et al. [2018] for survey), but less attention is given to extracting information (often, numeric) conveyed in tables. Tables may express performance of an algorithm on a dataset, report quantitative results of clinical trials, or describe compositions and properties of materials studied in a paper. Due to the importance of such information, we posit that IE from tables is essential for a comprehensive machine understanding of a given paper, and for increasing the coverage of resulting KBs.

We are motivated by curating a KB of all materials known to mankind (such as glasses, alloys), along with their properties. A preliminary analysis of material science (MatSci) papers reveals that around 85% of material compositions and their associated quantitative properties (e.g., hardness, viscosity, conductivity) are reported in tables. Our paper studies the first part of this IE problem – extraction of materials (IDs used in the paper), along with their constituents and relative percentages. For instance, Fig. 1a should output four materials (A1-A4), where ID A1 is associated with three constituents (MoO_3 , Fe_2O_3 , and P_2O_5) and their percentages, 5, 38, and 57, respectively. While not our focus, this

Sample Code	A1	A2	A3	A4	Glass composition in the paper: $20La_2S_3 - (80 - x)Ga_2S_3 - xCsCl$			Composition	$\log \sigma_{298}$ (S cm ⁻¹)	
Batch	MoO ₃	5	10	15	20	Glass	CsCl (mol%)	n (1.5 μ m)	(80GeS ₂ -20Ga ₂ S ₃) ₉₀ -(LiI) ₁₀	-6.34 (5)
Composition (mol %)	Fe ₂ O ₃	38	36	34	32	GLSC10	10	2.253 \pm 0.001	(80GeS ₂ -20Ga ₂ S ₃) ₉₀ -(NaCl) ₁₀	-6.92 (5)
	P ₂ O ₅	57	54	51	48	GLSC20	20	2.265 \pm 0.001	(80GeS ₂ -20Ga ₂ S ₃) ₉₀ -(NaI) ₁₀	-7.24 (3)
Molar ratio	Mo/P	0.04	0.09	0.15	0.21	GLSC30	30	2.322 \pm 0.001	(72GeS ₂ -28Ga ₂ S ₃) ₉₀ -(Li ₂ S) ₁₀	-5.74 (3)
	O/P	3.6	3.8	3.9	4.1	GLSC40	40	2.379 \pm 0.001		
	Fe/P	0.67	0.67	0.67	0.67					

Figure 1: Examples of composition tables (a) Multi-cell complete-info composition table Moguš-Milanković et al. [2003] (b) Multi-cell partial-info composition table Marmolejo et al. [1999] (c) Single-cell composition table Brehault et al. [2014]

extraction problem is also relevant for several other domains such as biomedical (drug compositions), environmental science (aerosols, air pollution, solid waste), and chemistry (polymers, colloidal gels).

Our preliminary analysis of composition tables reveals that MatSci researchers can express the same composition in a wide-variety of table styles. Two main types are *multi-cell compositions* (MCC), where material composition and constituents are on two axes and each cell represents the percentage (Figure 1a), and *single-cell compositions* (SCC), where the full composition is mentioned in a single cell as an expression (see Figure 1c). However, there are several other types – sometimes, the table has incomplete information and other default constituents are listed in caption or text (Figure 1b), or the table may mix composition and properties, or the caption may define composition in terms of mathematical variables and the table expresses the variable values per material. Additionally, there can be four units for specifying the percentage – mol percent, mol fraction, weight percent or weight fraction, requiring normalization. Interestingly, some researchers write percentages such that they add to numbers less than or more than 100, and expect the reader to re-normalize. All these and more make the problem of extracting material compositions from scientific tables a challenging problem.

In response, we first harvest a distantly supervised training dataset for the novel ML task. We match a manually-curated KB of materials and compositions with tables in the relevant papers, to automatically provide distantly-supervised labels for extraction (hand-annotated for dev/test sets). This results in a dataset of 5,883 tables, of which 2,355 express compositions, with 16,729 materials, and a total of 58,481 (material ID, constituent, composition percentage, unit) tuples. Existing table processing literature is not well-suited for our task, because it generally assumes prior knowledge of table structure and format, understanding which, as described above, is a key challenge for our task. In response, our baseline system DISCOMAT uses a pipeline of a domain-specific language model Gupta et al. [2022], and two graph neural networks (GNNs), along with several hand-coded features and constraints. We evaluate our system on accuracy metrics for various subtasks, including ID prediction, tuple-level prediction, material-level complete prediction. We find that DISCOMAT with constraints and features obtains upto 14 point increase in various accuracy numbers, compared to a model that uses vanilla GNNs. Our GNN-based architecture outperforms a recent table processor, which linearizes the table for prediction by a language model Herzig et al. [2020], by a wide margin. Subsequent analysis reveals common sources of DISCOMAT errors, which will inform future research.

2 Related work

Recent work has developed neural models for various NLP tasks based on tabular data, for instance, tabular natural language inference Orihuela et al. [2021], Minhas et al. [2022], QA over one or a corpus of tables Herzig et al. [2020], Yin et al. [2020], Arik and Pfister [2021], Glass et al. [2021], Pan et al. [2021], Chemmengath et al. [2021], table orientation classification Habibi et al. [2020], Nishida et al. [2017], and relation extraction from tables Govindaraju et al. [2013], Macdonald and Barbosa [2020]. Several papers study QA models. For instance, TaPas Herzig et al. [2020] linearizes a table and passes it to a BERT-based model pre-trained on Wikipedia tables – it answers NL questions over tables by selecting table cells and aggregation operators. TaBERT Yin et al. [2020] uses a different pre-training objective and model architecture to jointly learn NL sentence and table representations. Row and column intersection (RCI) model Glass et al. [2021] predicts the probability of finding the answer to a given question in each row and column of a table independently, without any pre-training on tables. TaPEX Liu et al. [2022] uses a BART encoder-decoder architecture, pre-trained via synthetic executable programs to mimic the behaviour of SQL execution engine. TABBIE Iida et al. [2021] consists of two transformers that encode rows and columns independently and is pre-trained

using the corrupt-cell objective. Similar to our work, tables have also been modeled as graphs for sequential question answering over tables Müller et al. [2019]. However, all these works generally assume a fixed and known structure of tables with the same orientation, with the top row being the header row in all cases – an assumption violated in our setting.

Orientation and semantic structure classification: DeepTable Habibi et al. [2020] is a permutation-invariant neural model, which classifies tables into three orientations, while TabNet Nishida et al. [2017] uses RNNs and CNNs in a hybrid fashion to classify web tables into five different types of orientations. InfoTabS Gupta et al. [2020] studies natural language inference on tabular data. Here, concatenated premise-hypothesis pair is sent through language models to classify whether the premise (info-box) entails, contradicts, or is unrelated to a given hypothesis. This has been extended to the multilingual setting Minhas et al. [2022], and has been combined with knowledge graphs Varun et al. [2022]. Some earlier works also focused on annotating column types, cells with entity IDs, pair of columns with binary relations, based on rule-based and other ML approaches, given a catalog consisting of types, entities and relations Limaye et al. [2010].

NLP for materials literature: After the success of BERT Devlin et al. [2019], numerous domain-specific language models have been released for public-use. For MatSci domain, researchers have contributed language models like MatSciBERT Gupta et al. [2022], MatBERT Trewartha et al. [2022], and BatteryBERT Huang and Cole [2022]. MatBERT Trewartha et al. [2022] highlights the advantages of materials domain-specific pre-training on the NER task. BatteryBERT exhibits superior performance on battery related downstream tasks. MatSciBERT yields state of the art performance on downstream tasks of abstract classification, NER, and relation classification, and we use it in our work. Wang et al. Wang et al. [2022] recently develop a rule-based NER and relation extraction to create a pipeline for extracting superalloy data from text and tables. There also exists a table extraction tool that takes input HTML or XML of MatSci research papers, and uses regular expression based parser for extracting compositions, scientific units, and related information Jensen et al. [2019]. However, the regexes used in these works are highly specific and will require significant modifications for different classes of materials. Despite the availability of MatSci language models, deep neural models have not been explored for IE from materials tables – the focus of this work.

3 Challenges in composition extraction from tables

We analyze numerous composition tables in MatSci research papers (see Figures 1, 2 and 5 for examples), and find that the task has several facets, with many table styles for similar compositions. We now describe the key challenges involved in the task of composition extraction from tables.

1. **Distractor rows and columns:** Additional information such as material properties, molar ratios, std errors in the same table. E.g., Figure 1a, last three rows are distractor rows.
2. **Orientation of tables:** Table shown in Figure 5a is a row oriented table—different compositions are written in different rows. Table in Figure 1a is a column oriented table.
3. **Different units:** Compositions can be in different units such as mol%, weight%, mol fraction, weight fraction. Some tables express a composition in both molar and mass units.
4. **Material IDs:** Authors refer to different materials in their publication by assigning them unique IDs. These material IDs may not be specified every time, (e.g., Figure 1c).
5. **Single-cell compositions (SCC):** In Figure 1a, all compositions are present in multiple table cells. Some authors report the entire composition in single table cell, as shown in figure 1c.
6. **Percentages exceeding 100:** Sum of coefficients may exceed 100, and re-normalization is needed. A common case is when a dopant is used; its amount is reported in excess of 100.
7. **Percentages as variables:** Contributions of constituents may be expressed using variables like x, y . In figure 2, x represents the mol% of (GeBr_4) and the 2nd row contains its value.
8. **Partial-information tables:** It is also common to have percentages of only some constituents in the table; the remaining composition is to be inferred based on paper text or table caption, e.g., Figure 1b. Another example: if the paper is on silicate glasses, then SiO_2 is assumed.
9. **Other corner cases:** There are several other corner cases like percentages missing from the table, compounds with variables (e.g., R_2O in header; value of R to be inferred from material ID), and highly unusual placement of information (some examples in appendix).

4 DISCOMAT architecture

To address these challenges, we present an ML formulation of the problem. Formally, given a table T , its caption, and the complete text of publication in which T occurs, we aim to extract compositions expressed in T , in the form $\{(id, c_k^{id}, p_k^{id}, u_k^{id})\}_{k=1}^{K^{id}}$. Here, id represents the material ID, as defined in the paper. Material IDs are defined by MatSci researchers to succinctly refer to that composition in text and other tables. c_k^{id} is a constituent element or compound present in the material, K^{id} is the total number of constituents in the material, $p_k^{id} > 0$ denotes the percentage contribution of c_k^{id} in its composition, and u_k^{id} is the unit of p_k^{id} (either mole% or weight%).

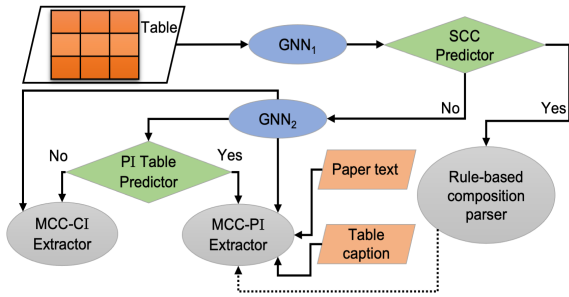


Figure 3: The design of DISCOMAT

IDs, constituents, and others. If no constituents or composition predictions are found, then T is deemed to be a non-composition (NC) table. Or else, it is an MCC table, for which DISCOMAT predicts whether it has all information in T or some information is missing (partial-information predictor). If it is complete information table, then GNN_2 's predictions are post-processed into compositions. If not, the caption and text of paper are also processed, along with GNN_2 's predictions lead to final composition extraction. We note that our system ignores statistically infrequent corner cases, such as single-cell partial information tables – we discuss this further in our error analysis. We now describe each component, one by one.

4.1 Graph neural networks for table processing

At the core of DISCOMAT are two GNNs that learn representations for each cell, row, column and the whole table. Let table T has R rows, C columns, and text at $(i, j)^{th}$ cell be t_{ij} , where $1 \leq i \leq R$, and $1 \leq j \leq C$. We construct a graph $G_T = (V_T, E_T)$, where V_T has a node for each cell (i, j) , one additional node for each row and column, denoted by $(i, 0)$ and $(0, j)$, respectively, and one node for the whole table represented by $(0, 0)$. The edges in E_T are directed. There are edges between a pair of nodes (in both directions) if they have the same row or same column. All the cell nodes have directed edges to the table node and also their corresponding row and column nodes. We initialize the embeddings \vec{x}_{ij} for each node (i, j) as follows. The table, row and column embeddings are randomly-initialized with a common vector, which gets trained during learning. Other nodes are associated with text t_{ij} – their embeddings are initialized by running a language model LM over t_{ij} .

As constructed, G_T is permutation-invariant, i.e., if we permute rows or columns, we get the same graph and same embeddings. However, initial rows/columns can be semantically different, since they often represent headings for the subsequent list. For instance, material IDs are generally mentioned in first one or two rows/columns of the table. So, we additionally define *index embeddings* \vec{p}_i to represent a row/column numbered i . We use the same index embeddings for rows and columns so that our model stays transpose-invariant. We also observe that while first few indices are different, the semantics is generally uniform for indices higher than 3. So, to allow DISCOMAT to handle large tables, we simply use $\vec{p}_i = \vec{p}_3 \forall i > 3$. Finally, some manually-defined features may be added to each node. The feature values are embedded as \vec{f} and concatenated to the cell embeddings. Combining

	$(GeSe_2)_{1-x}(GeBr_4)_x$		$(GeSe_2)_{1-x}Br_x$		
x	0.079	0.167	0.265	0.250	0.429
$p_{Se}(\%)$	94.1	86.0	76.5	84.1	78.0
	(92.1)	(83.3)	(73.5)	(91.7)	(81.2)
$p_{Br}(\%)$	5.8	14.0	23.5	15.9	22.0
	(7.9)	(16.7)	(26.5)	(8.3)	(18.8)

Figure 2: Percentages as variables Uemura et al. [2001]

Figure 3 illustrates the basic pipeline for extraction in DISCOMAT. We find that the simplest task is to identify whether the table T is an SCC table, owing to a distinctive presence of multiple numbers, and compounds in single cells. DISCOMAT first runs a GNN-based SCC predictor, which classifies T as an SCC table or not. For SCC table, it uses a standalone rule-based composition parser. For the other category, DISCOMAT runs a second GNN (GNN_2), and first labels rows and columns of T as compositions, material

all ideas, a cell embedding is initialized as:

$$\vec{x}_{ij} = \vec{f}_{ij} \parallel (LM_{CLS}(\langle CLS \ t_{ij} \ SEP \rangle) + \vec{p}_i + \vec{p}_j) \quad [1 \leq i \leq R, 1 \leq j \leq C].$$

Here, \parallel is the concat operation and LM_{CLS} gives the contextual embedding of the CLS token after running a LM over the sentence inside $\langle \rangle$. Message passing is run on the graph G_T using a GNN, which computes a learned feature vector \vec{h} for every node: $\{\vec{h}_{ij}\}_{i,j=(0,0)}^{(R,C)} = GNN(\{\vec{x}_{ij}\}_{i,j=(0,0)}^{(R,C)})$.

4.2 Single-cell composition tables

In its pipeline, DISCOMAT first classifies whether T is an SCC table. For that, it runs a GNN (named GNN_1) on T , as discussed above, with two manually defined features (discussed below). It then implements a Multi-layer Perceptron MLP_1 over the table-level feature vector \vec{h}_{00} to make the prediction. Additionally, GNN_1 also feeds row and column vectors \vec{h}_{i0} and \vec{h}_{0j} through another MLP (MLP_2) to predict whether they contain material IDs or not. If T is predicted as an SCC table, then one with the highest MLP_2 probability is deemed as material ID row/column (provided that probability > 0.5), and its contents are extracted as potential material IDs. If all row and column probabilities are less than 0.5, then table is predicted to not have Material IDs, as in Figure 1c.

Rule-based composition parser: For an SCC table, DISCOMAT must parse the full *composition expression* written in a single cell in the row/column corresponding to each Material ID. Such compositions are close to regular languages and can be parsed via regular expressions. Figure 4 shows the regular expression (simplified, for understandability) implemented in DISCOMAT. Here CMP denotes the matched composition, PATs are three main patterns for it, CSTs are sub-patterns, CPD is a compound, NUM is a number, OB and CB are, respectively, open and closed parentheses (or square brackets). W is zero or more whitespace characters, and SEP contains explicit separators like '-' or '+'. START and END are indicators to separate a regular expression from rest of the text.

CMP = PAT₁ | PAT₂ | PAT₃
 PAT_i = START CST_i (SEP CST_i)⁺ END
 CST₁ = NUM? W CPD
 CST_t = CST_t (SEP CST_t)^{*}
 CST₂ = (CST_t | OB CST_t CB) W NUM
 CST₃ = NUM W (CST_t | OB CST_t CB)

Figure 4: Regexes in composition parser

The first pattern parses simple number-compound expressions like $40\text{Bi}_2\text{O}_3 * 60\text{B}_2\text{O}_3$. Here each of the two constituents will match with CST_1 . The other two patterns handle *nested* compositions, where simple expressions are mixed in a given ratio. The main difference between second and third pattern is in the placement of outer ratios – after or before the simple composition, respectively. Example match for PAT_2 is $(40\text{Bi}_2\text{O}_3+60\text{B}_2\text{O}_3)30 - (\text{AgI}+\text{AgCl})70$, and for PAT_3 is $40\text{Bi}_2\text{O}_3,40\text{B}_2\text{O}_3,20(\text{AgI}:2\text{AgCl})$.

To materialize these rules, DISCOMAT pre-labels compounds. For our dataset, we use a list-based extractor, though other chemical data extractors Swain and Cole [2016] may also be used. After parsing, DISCOMAT normalizes all coefficients so that they sum to hundred. For nested expressions, the outer ratio and the inner ones are normalized separately and then multiplied. For units, DISCOMAT searches for common unit keywords such as mol, mass, weight, and their abbreviations like wt.%, and at.%. The search is done iteratively with increasing distance from cell containing the composition. If not found in the table, then the caption is searched. If still not found, mole% is used as default.

Manual Features: GNN_1 uses two hand-coded features. The first feature is set to true if that cell contains a composition that matches our rule-based composition parser. Each value, true or false, is embedded as $\vec{\sigma}$. The second feature named *max frequency feature* adds the bias that material IDs are generally unique in a table. We compute q_i^r and q_j^c , which denote the maximum frequency of any non-empty string occurring in the cells of row i and column j , respectively. If these numbers are on the lower side, then that row/column has more unique strings, which should increase the probability that it contains material IDs. The computed q values are embedded in a vector as \vec{q} . The embedded feature \vec{f}_{ij} for cell (i, j) is initialized as $\vec{\sigma}_{ij} \parallel (\vec{q}_i^r + \vec{q}_j^c)$.

	3	2	2	2	2	0	
0	Sample	PbO	B ₂ O ₃	P ₂ O ₅	TeO ₂	$\rho \pm 0.02$	
0		(mol%)					[g·cm ⁻³]
1	LBPT0	50	10	40	0	4.97	
1	LBPT1	45	9	36	10	5.14	
1	LBPT2	40	8	32	20	5.16	
1	LBPT3	35	7	28	30	5.19	
1	LBPT4	30	6	24	40	5.31	

	2	2	0	0	0	0
0	y	x	N _{Na}	T _g	C _Q (BO _{3A})	δ_{CS} (BO _{3A})
0			(10 ²⁷ m ⁻³)	(K)	(MHz)	(ppm)
1	0.2	0	0	707.3	2.49	16.4
1	0.2	0.2	1.35	690.1	2.51	16.3
1	0.2	0.4	2.84	695.3	2.50	16.2
1	0.2	0.6	4.42	719.4	2.49	16.2
1	0.2	0.8	6.03	731.9	2.50	16.5

Figure 5: Multi-cell composition tables (a) Complete information Koudelka et al. [2014] (b) Partial information Epping et al. [2005]

4.3 Multi-cell composition tables

If T is predicted to not be an SCC table, DiSCoMAT runs it through another GNN (GNN₂). The graph structure is very similar to G_T from Section 4.1, but with two major changes. First, a new *caption node* is created with initial embedding as given by LM processing the caption text. Edges are added from caption node to all row and column nodes. To propagate the information further to cells, edges are added from row/column nodes to corresponding cell nodes. The caption node especially helps in identifying non-composition (NC) tables. Second, the max frequency feature from Section 4.2 is also included in this GNN.

We use tables in Figure 5 as our running examples. Notice that Figure 5a is a complete-information table, whereas Figure 5b is not, and can only be understood in the context of its caption, which describes the composition as $[(Na_2O)_x(Rb_2O)_{1-x}]_y(B_2O_3)_{1-y}$. Here x, y are variables, which also need to be extracted and matched with the caption. DiSCoMAT first decodes the row and column feature vectors \vec{h}_{i0} and \vec{h}_{0j} , as computed by GNN₂, via an MLP₃ into four classes: composition, constituent, ID, and other (label IDs 1, 2, 3, 0, respectively). The figures illustrate this labeling for our running example. The cell at the intersection of composition row/column and constituent column/row contains the percentage contribution of that constituent in that composition.

Further, to associate the identified percentage contribution with the corresponding constituent (like P₂O₅ in Figure 5a) or variables x, y in Figure 5b), we perform classification at the edge level. For ease of exposition, we describe our method in this Section 4.3 for the setting that the table has been predicted by GNN₂ to have row-wise orientation, i.e., rows are compositions and columns are constituents. A transposed computation is done in the reverse case. Since the constituent/variable will likely occur in the same column or row as the cell containing percentage contribution, our method computes an edge feature vector: for edge $e = (i, j) \rightarrow (i', j')$, s.t. $i = i' \vee j = j'$, the feature vector $\vec{h}_e = \vec{h}_{ij} \parallel \vec{h}_{i'j'}$. It then takes all such edges e from cell (i, j) , if row i is labeled composition and column j is labeled constituent. Each edge e is classified through an MLP₄, and the edge with maximum logit value is picked to identify constituent/variable. This helps connect 36 to P₂O₅ and 0.8 to x in our running examples.

GNN₂ also helps in predicting NC tables. In case none of the rows/columns are predicted as 1 or 2, then the table is deemed as non-composition and discarded.

Partial information table predictor: Next, DiSCoMAT distinguishes between complete-information (CI) and partial-information (PI) MCC tables. It uses a logistic regression model with custom input features for this prediction task. Let P and Q be the sets of all row indices with label 1 (composition) and column indices with label 2 (constituent), respectively. Also, assume n_{ij} is the number present in table cell (i, j) or 0 if no number is present. To create the features, we first extract all the constituents (compounds) and variables predicted by MLP₄. We now construct five table-level features (F1-F5). F1 and F2 count the number of unique variables and chemical compounds extracted by MLP₄. The intuition is that F1 is high, then it is more likely an MCC-PI, and vice-versa if F2 is high. F3 computes the number of rows and columns labeled as 2 (constituent) by MLP₃. The more the value of F3, the more likely it is that the table is MCC-CI. Features F4 (and F5) computes the maximum (average) of the sum of all extracted compositions. The intuition of F4 and F5 is that the higher these feature values, higher the chance of the table being an MCC-CI. Formally,

$$F4 = \left(\max_{i \in P} \sum_{j \in Q} n_{ij} \right) \quad F5 = \left(\frac{1}{|P|} \sum_{i \in P} \sum_{j \in Q} n_{ij} \right).$$

MCC table extractor: For MCC-CI, MLP_3 and MLP_4 outputs are post-processed, and units are added (similar to SCC tables), to construct final extracted tuples. For MCC-PI, on the other hand, information in text needs to be combined with the MLP outputs for final extraction. The first step here is to search for the composition expression, which may be present in table caption, table footer, and if not there, in somewhere in the rest of the research paper. Here, DISCOMAT resorts to using our rule-based composition parser from Figure 4, but with one key difference. Now, the composition may contain variables (x, y) and even mathematical expressions like $100 - x$. So the regular grammar is enhanced to replace the non-terminal NUM with a non-terminal EXPR, which represents, numbers, variables, and simple mathematical expressions over them. An added constraint is that if there are variables in set Q , then those variables must be present in the matched composition expression. DISCOMAT completes the composition by substituting the variable values from every composition row into the matched composition. There may be other types of MCC-PI tables where only compounds are identified in tables, such as Figure 1b. For these, DISCOMAT first computes the constituent contributions in terms of variables from composition expression, and then equates it with the numbers present in rows/columns labeled 1 (composition). In our example, DISCOMAT matches x with the numbers 10, 20, 30, and 40, and the rest of the composition is extracted by processing the composition expression in the caption with these values of x . Units and material IDs are added to the tuples, similar to other tables.

4.4 Loss functions & constraint-aware training

DISCOMAT needs to train the two GNNs and the PI table predictor. Our data construction provides gold labels for each prediction task (discussed in next section), so we train these component-wise. The PI table predictor is trained on standard logistic regression loss. GNN_1 is trained on a weighted sum of binary cross entropy loss for SCC table classification and row/column classification for material IDs – weight is a hyper-parameter. Similarly, GNN_2 loss function consists of sum of row/column cross-entropy loss and edge binary cross-entropy loss.

GNN_2 has the more complex prediction problem, since it has to perform four-way labeling for each row and column. In initial experiments, we find that the model sometimes makes structural errors like labeling one row as constituent and another row as composition in the same table – highly unlikely as per the semantics of composition tables. To encourage GNN_2 to make structurally consistent predictions, we express a set of constraints on the complete labelings, as follows. (1) A row and a column cannot both have compositions or constituents. (2) Composition and material ID must be orthogonally predicted (i.e, if a row has a composition then ID must be predicted in some column, and vice versa). (3) Constituents and material IDs must never be orthogonally predicted (if rows have constituents then another row must have the ID). And, (4) material ID must occur at most once for the entire table. Limitation of space precludes complete mathematical exposition of all constraints (see Appendix for details). As an example, constraint (1) can be expressed as a hard constraint as:

$$r_i = l \Rightarrow c_j \neq l \quad \forall i \in \{1, \dots, R\}, j \in \{1, \dots, C\}, l \in \{1, 2\}.$$

Here, r_i and c_j are predicted labels of row i and column j . We wish to impose these structural constraints at training time, so that the model is trained to honor them. We follow prior work by Nandwani et al. [2019], to first convert these hard constraints into a probabilistic statement. For example, constraint (1) gets expressed as:

$$P(r_i = l; \theta) + P(c_j = l; \theta) - 1 \leq 0 \quad \forall i \in \{1, \dots, R\}, j \in \{1, \dots, C\}, l \in \{1, 2\}.$$

θ represents GNN_2 's parameters. Following same work, each such constraint gets converted to an auxiliary penalty term, which gets added in the loss function for constraint-aware training. The first constraint gets converted to:

$$\lambda \sum_{i=1}^R \sum_{j=1}^C \sum_{l=1}^2 \max(0, P(r_i = l; \theta) + P(c_j = l; \theta) - 1)$$

This (and similar auxiliary losses for other constraints) get added to the GNN_2 's loss function for better training. λ is a hyper-parameter. Note that we also use constraint (4) for GNN_1 training.

5 Experiments

Dataset construction: Our goal is create a train set with table-level annotation (NC, SCC, MCC-PI, MCC-CI), row/column-level annotation (ID, composition, constituent, other), and edge level

annotation. We also create dev/test sets with these and final tuple-level ground truth. For training set, we use the InterGlad database New Glass Forum [2019] – a commercial DB of glass compositions, associated with paper references, from where these compositions were manually copied in DB. Separately, we extract all tables from 2,536 papers (using Elsevier API) found in InterGlad. We use table parser Jensen et al. [2019] to parse raw tables and captions from XML. We keep 1,880 papers for train set, and rest are split in dev and test.

Note that the DB does not contain information about where exactly a given composition appears in the paper – in text, images, graphs or tables. If it is present in a table, it can appear in any column or row. Knowing the exact location of composition requires significant manual annotation, so we use distantly supervised train set construction Mintz et al. [2009]. The first step is to simply match the chemical compounds and percentages (or equivalent fractions) mentioned in the DB with the text in a table from the associated paper. If composition percentages are found completely and in multiple cells of the table, it is marked as MCC-CI. However, due to various problems identified in Section 3, it will miss many composition tables. To increase the coverage, we additionally use our rule-based composition parser, but restricted to only those compounds (CPD non-terminal in Figure 4) that appear in the DB for this paper. This is important supervision, and leads to a high quality annotation of composition expressions in these papers. If this matching happens in a table cell, the table is deemed as SCC. If it is matched with caption/paper text that has a variable (or compound) that is found in the table, it is marked as MCC-PI. If no matching occurs, then the table is marked as NC. This automatic annotation is post-processed into row, column and edge labels. One further challenge is that material IDs in DB are global, and unique across all papers; they often differ from the local IDs mentioned in papers. So, we manually annotate material IDs for all the identified composition tables in the training set. This leads to a train set of 11,207 materials with 38,799 tuples from 4,408 tables.

Since train set is distantly supervised and can have noise, a MatSci expert manually annotated the dev and test tables with row/column/edge labels, units, tuples, compositions, and table type, resulting in over 2,500 materials and over 9,500 tuples per set. Further statistics are discussed in Appendix.

Baseline models: We implement DISCOMAT with *LM* as MatSciBERT Gupta et al. [2022], and the GNNs as Graph Attention Networks Veličković et al. [2018]. We compare DISCOMAT with two non-GNN baseline models. Our first baseline is TAPAS Herzig et al. [2020], a state-of-the-art table QA system, which flattens the table, adds row and column index embeddings, and passes as input to a language model. To use TaPas for our task, we use table caption as proxy for the input question. All the model parameters in this setting are initialized randomly. Our second baseline is TAPAS-ADAPTED, with the goal of providing the benefit of MatSciBERT to TAPAS – it initializes language model weights by MatSciBERT. For the input to remain consistent with MatSciBERT, we add row and column index embeddings to MatSciBERT *output*, instead of input as in original TAPAS model. Appendix has further details on TAPAS models.

Evaluation metrics: We compute several metrics in our evaluation. (1) *Table-type (TT) prediction accuracy* – it computes table-level accuracy on the 4-way table classification as NC, SCC, MCC-CI and MCC-PI. (2) *ID F_1 score* computes F_1 score for Material ID extraction. (3) *Tuple-level (TL) F_1 score* evaluates performance on the extraction of composition tuples. A gold is considered matching with a predicted 4-tuple if *all* arguments match exactly. (4) *Material-level (MatL) F_1 score* is the strongest metric. It evaluates whether all predicted information related to a material (including its ID, all constituents and their percentages) match exactly with the gold. Finally, (5) *constraint violations (CV)* counts the number of violations of hard constraints in the prediction. We consider all four types of constraints, as discussed in Section 4.4.

Implementation details: For Graph Attention Networks (GATs) Veličković et al. [2018], we use the GAT implementation of Deep Graph Library Wang et al. [2019]. For LMs and TAPAS, we use the implementation by Transformers library Wolf et al. [2020]. We implement and train all models using PyTorch Paszke et al. [2019]. We optimize the model parameters using Adam Kingma and Ba [2015] and a triangular learning rate Smith [2017]. We further use different learning rates for *LM* and non-LM parameters (GNNs, MLPs). To deal with imbalanced labels, we scale loss for all labels by weights inversely proportional to their frequency in the training set. All experiments were run on a machine with one 32 GB V100 GPU. Each model is run with three seeds and the mean and std. deviation are reported.

5.1 Results

How does table linearization compare with a graph-based model for our task? To answer this question, we compare DiSCoMAT with two TAPAS-based models. Since the baselines do not have the benefit of regular expressions, features, and constraints, we implement a version of our model without these, which we call v-DiSCoMAT. We do this comparison, trained and tested only on the subset of MCC-CI and NC tables, since other table types require regular expressions for processing. As shown in Table 1 v-DiSCoMAT obtains 6-7 pt higher F_1 on TL and MatL scores, suggesting that a graph-based extractor is likely a better fit for our problem - this led to us choosing a GNN-based approach for DiSCoMAT.

Table 1: Performance of v-DiSCoMAT vs baseline models on MCC-CI and NC table types

Model	ID F_1	TL F_1	MatL F_1	CV
TAPAS	80.37 (\pm 4.78)	71.23 (\pm 0.77)	49.88 (\pm 0.10)	543.67
TAPAS-ADAPTED	89.65 (\pm 0.46)	70.91 (\pm 3.79)	57.88 (\pm 2.73)	490.33
v-DiSCoMAT	77.38 (\pm 12.21)	76.52 (\pm 2.37)	64.71 (\pm 3.45)	626.33

How does DiSCoMAT model perform on the complete task? Table 2, reports DiSCoMAT performance on the full test set with all table types. Its ID and tuple F_1 -scores are 82 and 70, respectively. Since these errors get multiplied, unsurprisingly, its material-level F_1 -score is lower (63.5). Table 3 reports DiSCoMAT performance for different table types. In this experiment, we assume that table type is already known and run only the relevant part of DiSCoMAT for extraction. We find that MCC-PI is the hardest table type, since it requires combining information from text and tables for accurate extraction. A larger standard deviation in ID F_1 for MCC-PI is attributed to the fact that material IDs occur relatively rarely for this table type – the test set for MCC-PI consists of merely 20 material ID rows and columns.

Table 2: Contribution of task specific features and constraints in DiSCoMAT.

Model	TT Acc.	ID F_1	TL F_1	MatL F_1	CV
DiSCoMAT	88.35 (\pm 1.20)	82.40 (\pm 3.88)	70.14 (\pm 0.44)	63.51 (\pm 1.90)	87.33
DiSCoMAT w/o features	88.84 (\pm 1.00)	80.80 (\pm 3.24)	68.60 (\pm 1.26)	62.53 (\pm 1.89)	120.11
DiSCoMAT w/o constraints	88.47 (\pm 0.31)	78.71 (\pm 3.66)	69.28 (\pm 1.11)	60.94 (\pm 0.98)	584.78
DiSCoMAT w/o captions	87.35 (\pm 0.71)	84.23 (\pm 0.51)	67.51 (\pm 1.36)	63.50 (\pm 2.49)	19.11
v-DiSCoMAT	88.59 (\pm 0.33)	68.54 (\pm 9.32)	65.98 (\pm 1.21)	59.36 (\pm 2.20)	541

Table 3: Performance of DiSCoMAT on different table types

Table Type	ID F_1	TL F_1	MatL F_1	CV
SCC	88.81 (\pm 1.54)	79.89 (\pm 0.18)	78.21 (\pm 0.14)	0.67
MCC-CI	93.91 (\pm 1.46)	77.62 (\pm 1.07)	65.41 (\pm 4.35)	59.33
MCC-PI	70.67 (\pm 11.58)	50.60 (\pm 2.59)	51.66 (\pm 2.21)	26.67

What is the incremental contribution of task-specific features and constraints? Table 2 also presents the ablation experiments. DiSCoMAT scores much higher than v-DiSCoMAT, which does not have these features and constraints. We also perform additional ablations removing one component at a time. Unsurprisingly constrained training helps with reducing constraint violations. Both constraints and features help with ID prediction, due to constraints (2), (3), (4) and max frequency feature. Removal of caption node significantly hurts performance on MCC-PI tables, as these tables require combining caption with table cells. All contribute to the tuple-level metric.

What are the typical errors in DiSCoMAT? Confusion matrix in Figure 6 suggests that most table type errors are between MCC-PI and NC tables. This could be attributed to following reasons. (i) DiSCoMAT has difficulty identifying rare compounds like Yb_2O_3 , $ErS_{3/2}$, Co_3O_4 found in MCC-PI—these aren’t present frequently in the training set. (ii) MCC-PI tables

True label	SCC	98	2	2	11
	MCC-CI	1	121	1	9
	MCC-PI	4	4	81	23
	NC	10	2	7	361
		SCC	MCC-CI	MCC-PI	NC
		Predicted label			

Figure 6: Confusion matrix for all table types

specify dopant percentages found in small quantities. (iii) Completion of composition in MCC-PI tables require other tables from the same publication. (iv) Finally, MCC-PI composition may contain additional information such as properties that may bias the model to classify it as an NC table.

6 Conclusions

We define the novel task of extracting material compositions from tables in scientific articles. We harvest a dataset using distant supervision, combining information from a manually developed database of materials with tables in respective papers. We present a strong baseline system, DISCOMAT, which is a pipeline of a material science language model, two graph neural networks along with task-specific regular expressions, features and constraints. Our experiments show much better performance than an alternative architecture that linearizes the tables. In the future, we plan to extend it to extracting material properties from tables.

DISCOMAT is a pipelined solution trained component-wise. This raises a research question: can we train one end-to-end trained ML model that not only analyzes a wide variety of table structures, but also combines understanding of regular expressions, extraction of chemical compounds and scientific units, text understanding and some mathematical processing. This defines a challenging ML research question, and one that can have direct impact to the scientific MatSci community.

References

- Sercan Ö. Arik and Tomas Pfister. TabNet: Attentive interpretable tabular learning. *Proceedings of the AAAI Conference on Artificial Intelligence*, 35(8):6679–6687, May 2021. URL <https://ojs.aaai.org/index.php/AAAI/article/view/16826>.
- Antoine Brehault, Solenn Cozic, Rémi Boidin, Laurent Calvez, Eugène Bychkov, Pascal Masselin, Xianghua Zhang, and David Le Coq. Influence of n_{ax} ($x = i$ or cl) additions on ges_2 – ga_2s_3 based glasses. *Journal of Solid State Chemistry*, 220:238–244, 2014.
- Saneem A. Chemmengath, Vishwajeet Kumar, Samarth Bharadwaj, Jaydeep Sen, Mustafa Canim, Soumen Chakrabarti, Alfio Gliozzo, and Karthik Sankaranarayanan. Topic transferable table question answering. In Marie-Francine Moens, Xuanjing Huang, Lucia Specia, and Scott Wen-tau Yih, editors, *Proceedings of the 2021 Conference on Empirical Methods in Natural Language Processing, EMNLP 2021, Virtual Event / Punta Cana, Dominican Republic, 7-11 November, 2021*, pages 4159–4172, 2021.
- Jacob Devlin, Ming-Wei Chang, Kenton Lee, and Kristina Toutanova. BERT: Pre-training of deep bidirectional transformers for language understanding. In *Proceedings of NAACL*, pages 4171–4186, Minneapolis, Minnesota, June 2019. Association for Computational Linguistics. doi: 10.18653/v1/N19-1423. URL <https://www.aclweb.org/anthology/N19-1423>.
- J.R. Duclère, A.A. Lipovskii, A.P. Mirgorodsky, Ph. Thomas, D.K. Tagantsev, and V.V. Zhurikhina. Kerr studies of several tellurite glasses. *Journal of Non-Crystalline Solids*, 355(43):2195–2198, 2009. ISSN 0022-3093. doi: <https://doi.org/10.1016/j.jnoncrysol.2009.07.022>. URL <https://www.sciencedirect.com/science/article/pii/S0022309309005109>.
- Jan Dirk Epping, Hellmut Eckert, Árpád W Imre, and Helmut Mehrer. Structural manifestations of the mixed-alkali effect: Nmr studies of sodium rubidium borate glasses. *Journal of non-crystalline solids*, 351(43-45):3521–3529, 2005.
- Patrick Ernst, Amy Siu, and Gerhard Weikum. Knowlife: a versatile approach for constructing a large knowledge graph for biomedical sciences. *BMC Bioinform.*, 16:157:1–157:13, 2015.
- Michael R. Glass, Mustafa Canim, Alfio Gliozzo, Saneem A. Chemmengath, Vishwajeet Kumar, Rishav Chakravarti, Avi Sil, Feifei Pan, Samarth Bharadwaj, and Nicolas Rodolfo Fauceglia. Capturing row and column semantics in transformer based question answering over tables. In *NAACL-HLT*, pages 1212–1224. Association for Computational Linguistics, 2021.
- Vidhya Govindaraju, Ce Zhang, and Christopher Ré. Understanding tables in context using standard nlp toolkits. In *Proceedings of the 51st Annual Meeting of the Association for Computational Linguistics (Volume 2: Short Papers)*, pages 658–664, 2013.

- Tanishq Gupta, Mohd Zaki, N. M. Anoop Krishnan, and Mausam. MatSciBERT: A materials domain language model for text mining and information extraction. *npj Computational Materials*, 8(1):102, May 2022. ISSN 2057-3960. doi: 10.1038/s41524-022-00784-w. URL <https://www.nature.com/articles/s41524-022-00784-w>.
- Vivek Gupta, Maitrey Mehta, Pegah Nokhiz, and Vivek Srikumar. INFOTABS: inference on tables as semi-structured data. In *ACL*, pages 2309–2324. Association for Computational Linguistics, 2020.
- Maryam Habibi, Johannes Starlinger, and Ulf Leser. Deeptable: a permutation invariant neural network for table orientation classification. *Data Mining and Knowledge Discovery*, 34(6):1963–1983, 2020.
- Thierry Hamon, Natalia Grabar, and Fleur Mouglin. Querying biomedical linked data with natural language questions. *Semantic Web*, 8(4):581–599, 2017.
- Jonathan Herzig, Pawel Krzysztof Nowak, Thomas Müller, Francesco Piccinno, and Julian Eisen-schlos. TaPas: Weakly supervised table parsing via pre-training. In *Proceedings of the 58th Annual Meeting of the Association for Computational Linguistics*, pages 4320–4333, Online, July 2020. Association for Computational Linguistics. doi: 10.18653/v1/2020.acl-main.398. URL <https://aclanthology.org/2020.acl-main.398>.
- Tom Hope, Aida Amini, David Wadden, Madeleine van Zuylen, Sravanthi Parasa, Eric Horvitz, Daniel S. Weld, Roy Schwartz, and Hannaneh Hajishirzi. Extracting a knowledge base of mechanisms from COVID-19 papers. In Kristina Toutanova, Anna Rumshisky, Luke Zettlemoyer, Dilek Hakkani-Tür, Iz Beltagy, Steven Bethard, Ryan Cotterell, Tanmoy Chakraborty, and Yichao Zhou, editors, *Proceedings of the 2021 Conference of the North American Chapter of the Association for Computational Linguistics: Human Language Technologies, NAACL-HLT 2021, Online, June 6-11, 2021*, pages 4489–4503. Association for Computational Linguistics, 2021.
- Shu Huang and Jacqueline M. Cole. Batterybert: A pretrained language model for battery database enhancement. *Journal of Chemical Information and Modeling*, 2022. doi: 10.1021/acs.jcim.2c00035. URL <https://doi.org/10.1021/acs.jcim.2c00035>.
- Hiroshi Iida, Dung Thai, Varun Manjunatha, and Mohit Iyyer. TABBIE: pretrained representations of tabular data. In *NAACL-HLT*, pages 3446–3456. Association for Computational Linguistics, 2021.
- Sergey Ioffe and Christian Szegedy. Batch normalization: Accelerating deep network training by reducing internal covariate shift. In *International conference on machine learning*, pages 448–456. PMLR, 2015.
- Anubhav Jain, Shyue Ping Ong, Geoffroy Hautier, Wei Chen, William Davidson Richards, Stephen Dacek, Shreyas Cholia, Dan Gunter, David Skinner, Gerbrand Ceder, et al. Commentary: The materials project: A materials genome approach to accelerating materials innovation. *APL materials*, 1(1):011002, 2013.
- Zach Jensen, Edward Kim, Soonhyoung Kwon, Terry Z. H. Gani, Yuriy Román-Leshkov, Manuel Moliner, Avelino Corma, and Elsa Olivetti. A machine learning approach to zeolite synthesis enabled by automatic literature data extraction. *ACS Central Science*, 5(5):892–899, 2019. doi: 10.1021/acscentsci.9b00193. URL <https://doi.org/10.1021/acscentsci.9b00193>.
- Nirmal Kaur, Atul Khanna, Marina González-Barriuso, Fernando González, and Banghao Chen. Effects of al₃₊, w₆₊, nb₅₊ and pb₂₊ on the structure and properties of borotellurite glasses. *Journal of Non-Crystalline Solids*, 429:153–163, 2015. ISSN 0022-3093. doi: <https://doi.org/10.1016/j.jnoncrysol.2015.09.005>. URL <https://www.sciencedirect.com/science/article/pii/S0022309315301824>.
- Diederik P. Kingma and Jimmy Ba. Adam: A method for stochastic optimization. In *ICLR (Poster)*, 2015.
- Ladislav Koudelka, Ivana Rösslerová, Zdeněk Černošek, Petr Mošner, Lionel Montagne, and Bertrand Revel. The structural role of tellurium dioxide in lead borophosphate glasses. *Journal of non-crystalline solids*, 401:124–128, 2014.

- Girija Limaye, Sunita Sarawagi, and Soumen Chakrabarti. Annotating and searching web tables using entities, types and relationships. *Proc. VLDB Endow.*, 3(1):1338–1347, 2010.
- Qian Liu, Bei Chen, Jiaqi Guo, Morteza Ziyadi, Zeqi Lin, Weizhu Chen, and Jian-Guang Lou. TAPEX: Table pre-training via learning a neural SQL executor. In *International Conference on Learning Representations*, 2022. URL <https://openreview.net/forum?id=050443AsCP>.
- Erin Macdonald and Denilson Barbosa. Neural relation extraction on wikipedia tables for augmenting knowledge graphs. In *Proceedings of the 29th ACM International Conference on Information & Knowledge Management, CIKM '20*, page 2133–2136, New York, NY, USA, 2020. Association for Computing Machinery. ISBN 9781450368599. URL <https://doi.org/10.1145/3340531.3412164>.
- EM Marmolejo, E Granado, OL Alves, CL Cesar, and LC Barbosa. Spectroscopy and thermal properties of Ga_2S_3 based glasses. *Journal of non-crystalline solids*, 247(1-3):189–195, 1999.
- David A McKeown, Wing K Kot, and Ian L Pegg. X-ray absorption studies of the local strontium environments in borosilicate waste glasses. *Journal of Non-Crystalline Solids*, 317(3):290–300, 2003. ISSN 0022-3093. doi: [https://doi.org/10.1016/S0022-3093\(02\)01816-1](https://doi.org/10.1016/S0022-3093(02)01816-1). URL <https://www.sciencedirect.com/science/article/pii/S0022309302018161>.
- Bhavnick Minhas, Anant Shankhdhar, Vivek Gupta, Divyanshu Aggarwal, and Shuo Zhang. XIn-foTabS: Evaluating multilingual tabular natural language inference. In *Proceedings of the Fifth Fact Extraction and VERification Workshop (FEVER)*, pages 59–77, Dublin, Ireland, May 2022. Association for Computational Linguistics. doi: 10.18653/v1/2022.fever-1.7. URL <https://aclanthology.org/2022.fever-1.7>.
- Mike Mintz, Steven Bills, Rion Snow, and Daniel Jurafsky. Distant supervision for relation extraction without labeled data. In *Proceedings of the Joint Conference of the 47th Annual Meeting of the ACL and the 4th International Joint Conference on Natural Language Processing of the AFNLP*, pages 1003–1011, Suntec, Singapore, August 2009. Association for Computational Linguistics. URL <https://aclanthology.org/P09-1113>.
- A Moguš-Milanković, A Šantić, A Gajović, and DE Day. Spectroscopic investigation of $\text{MgO}-\text{Fe}_2\text{O}_3-\text{P}_2\text{O}_5$ and $\text{SrO}-\text{Fe}_2\text{O}_3-\text{P}_2\text{O}_5$ glasses. part i. *Journal of non-crystalline solids*, 325(1-3):76–84, 2003.
- Thomas Müller, Francesco Piccinno, Peter Shaw, Massimo Nicosia, and Yasemin Altun. Answering conversational questions on structured data without logical forms. In *EMNLP/IJCNLP (1)*, pages 5901–5909. Association for Computational Linguistics, 2019.
- T. Murata, M. Sato, H. Yoshida, and K. Morinaga. Compositional dependence of ultraviolet fluorescence intensity of Ce^{3+} in silicate, borate, and phosphate glasses. *Journal of Non-Crystalline Solids*, 351(4):312–316, 2005. ISSN 0022-3093. doi: <https://doi.org/10.1016/j.jnoncrysol.2004.11.013>. URL <https://www.sciencedirect.com/science/article/pii/S0022309304010804>.
- Rahul Nadkarni, David Wadden, Iz Beltagy, Noah A. Smith, Hannaneh Hajishirzi, and Tom Hope. Scientific language models for biomedical knowledge base completion: An empirical study. In Danqi Chen, Jonathan Berant, Andrew McCallum, and Sameer Singh, editors, *3rd Conference on Automated Knowledge Base Construction, AKBC 2021, Virtual, October 4-8, 2021*, 2021.
- Yatin Nandwani, Abhishek Pathak, Mausam, and Parag Singla. A primal dual formulation for deep learning with constraints. In H. Wallach, H. Larochelle, A. Beygelzimer, F. d'Alché-Buc, E. Fox, and R. Garnett, editors, *Advances in Neural Information Processing Systems*, volume 32. Curran Associates, Inc., 2019.
- Zara Nasar, Syed Waqar Jaffry, and Muhammad Kamran Malik. Information extraction from scientific articles: a survey. *Scientometrics*, 117(3):1931–1990, 2018.
- Japan New Glass Forum. International glass database system, March 2019. URL https://www.newglass.jp/interglad_n/gaiyo/info_e.html.

- Kyosuke Nishida, Kugatsu Sadamitsu, Ryuichiro Higashinaka, and Yoshihiro Matsuo. Understanding the semantic structures of tables with a hybrid deep neural network architecture. In *Thirty-First AAAI Conference on Artificial Intelligence*, 2017.
- Refka Oueslati Omrani, Saida Krimi, Jean Jacques Videau, Ismail Khattech, Abdelaziz El Jazouli, and Mohamed Jemal. Structural investigations and calorimetric dissolution of manganese phosphate glasses. *Journal of Non-Crystalline Solids*, 389:66–71, 2014. ISSN 0022-3093. doi: <https://doi.org/10.1016/j.jnoncrysol.2014.02.006>. URL <https://www.sciencedirect.com/science/article/pii/S0022309314000957>.
- Mario Alberto Ramirez Orihuela, Alex Bogatu, Norman Paton, and André Freitas. Natural language inference over tables: Enabling explainable data exploration on data lakes. In *Eighteenth Extended Semantic Web Conference - Research Track*, 2021. URL <https://openreview.net/forum?id=11NA3w6pDG->.
- Feifei Pan, Mustafa Canim, Michael Glass, Alfio Gliozzo, and Peter Fox. CLTR: An end-to-end, transformer-based system for cell-level table retrieval and table question answering. In *Proceedings of the 59th Annual Meeting of the Association for Computational Linguistics and the 11th International Joint Conference on Natural Language Processing: System Demonstrations*, pages 202–209, Online, August 2021. Association for Computational Linguistics. doi: 10.18653/v1/2021.acl-demo.24. URL <https://aclanthology.org/2021.acl-demo.24>.
- Adam Paszke, Sam Gross, Francisco Massa, Adam Lerer, James Bradbury, Gregory Chanan, Trevor Killeen, Zeming Lin, Natalia Gimelshein, Luca Antiga, Alban Desmaison, Andreas Kopf, Edward Yang, Zachary DeVito, Martin Raison, Alykhan Tejani, Sasank Chilamkurthy, Benoit Steiner, Lu Fang, Junjie Bai, and Soumith Chintala. Pytorch: An imperative style, high-performance deep learning library. In *Advances in Neural Information Processing Systems 32*, pages 8024–8035. Curran Associates, Inc., 2019. URL <http://papers.neurips.cc/paper/9015-pytorch-an-imperative-style-high-performance-deep-learning-library.pdf>.
- Yong Beom Shin, Chang Kuk Yang, and Jong Heo. Optimization of dy³⁺-doped ge–ga–as–s–csbr glass composition and its 1.31 μm emission properties. *Journal of Non-Crystalline Solids*, 298(2): 153–159, 2002. ISSN 0022-3093. doi: [https://doi.org/10.1016/S0022-3093\(02\)00946-8](https://doi.org/10.1016/S0022-3093(02)00946-8). URL <https://www.sciencedirect.com/science/article/pii/S0022309302009468>.
- Leslie N. Smith. Cyclical learning rates for training neural networks. In *WACV*, pages 464–472. IEEE Computer Society, 2017.
- Nitish Srivastava, Geoffrey Hinton, Alex Krizhevsky, Ilya Sutskever, and Ruslan Salakhutdinov. Dropout: A simple way to prevent neural networks from overfitting. *Journal of Machine Learning Research*, 15(56):1929–1958, 2014. URL <http://jmlr.org/papers/v15/srivastava14a.html>.
- Matthew C. Swain and Jacqueline M. Cole. Chemdataextractor: A toolkit for automated extraction of chemical information from the scientific literature. *Journal of Chemical Information and Modeling*, 56(10):1894–1904, 2016. doi: 10.1021/acs.jcim.6b00207. URL <https://doi.org/10.1021/acs.jcim.6b00207>.
- Amalie Trewartha, Nicholas Walker, Haoyan Huo, Sanghoon Lee, Kevin Cruse, John Dagdelen, Alexander Dunn, Kristin A. Persson, Gerbrand Ceder, and Anubhav Jain. Quantifying the advantage of domain-specific pre-training on named entity recognition tasks in materials science. *Patterns*, 3(4):100488, 2022. ISSN 2666-3899. doi: <https://doi.org/10.1016/j.patter.2022.100488>. URL <https://www.sciencedirect.com/science/article/pii/S2666389922000733>.
- George Tsatsaronis, Georgios Balikas, Prodromos Malakasiotis, Ioannis Partalas, Matthias Zschunke, Michael R. Alvers, Dirk Weissenborn, Anastasia Krithara, Sergios Petridis, Dimitris Polychronopoulos, Yannis Almirantis, John Pavlopoulos, Nicolas Baskiotis, Patrick Gallinari, Thierry Artières, Axel-Cyrille Ngonga Ngomo, Norman Heino, Éric Gaussier, Liliana Barrio-Alvers, Michael Schroeder, Ion Androutsopoulos, and Georgios Paliouras. An overview of the BIOASQ large-scale biomedical semantic indexing and question answering competition. *BMC Bioinform.*, 16:138:1–138:28, 2015.

- Osamu Uemura, Takeshi Usuki, Masanori Inoue, Keigo Abe, Yasuo Kameda, and Masaki Sakurai. Local atomic order of ge–se–br glasses. *Journal of non-crystalline solids*, 293:792–798, 2001.
- Yerram Varun, Aayush Sharma, and Vivek Gupta. Trans-KBLSTM: An external knowledge enhanced transformer BiLSTM model for tabular reasoning. In *Proceedings of Deep Learning Inside Out (DeeLIO 2022): The 3rd Workshop on Knowledge Extraction and Integration for Deep Learning Architectures*, pages 62–78, Dublin, Ireland and Online, May 2022. Association for Computational Linguistics. doi: 10.18653/v1/2022.deelio-1.7. URL <https://aclanthology.org/2022.deelio-1.7>.
- Petar Veličković, Guillem Cucurull, Arantxa Casanova, Adriana Romero, Pietro Liò, and Yoshua Bengio. Graph Attention Networks. *International Conference on Learning Representations*, 2018. URL <https://openreview.net/forum?id=rJXmpikCZ>.
- Vineeth Venugopal, Suresh Bishnoi, Sourabh Singh, Mohd Zaki, Hargun Singh Grover, Mathieu Bauchy, Manish Agarwal, and NM Anoop Krishnan. Artificial intelligence and machine learning in glass science and technology: 21 challenges for the 21st century. *International journal of applied glass science*, 12(3):277–292, 2021.
- Minjie Wang, Da Zheng, Zihao Ye, Quan Gan, Mufei Li, Xiang Song, Jinjing Zhou, Chao Ma, Lingfan Yu, Yu Gai, Tianjun Xiao, Tong He, George Karypis, Jinyang Li, and Zheng Zhang. Deep graph library: A graph-centric, highly-performant package for graph neural networks. *arXiv preprint arXiv:1909.01315*, 2019.
- Weiren Wang, Xue Jiang, Shaohan Tian, Pei Liu, Depeng Dang, Yanjing Su, Turab Lookman, and Jianxin Xie. Automated pipeline for superalloy data by text mining. *npj Computational Materials*, 8(1):1–12, January 2022. ISSN 2057-3960. doi: 10.1038/s41524-021-00687-2. URL <https://www.nature.com/articles/s41524-021-00687-2>.
- Thomas Wolf, Lysandre Debut, Victor Sanh, Julien Chaumond, Clement Delangue, Anthony Moi, Pierric Cistac, Tim Rault, Rémi Louf, Morgan Funtowicz, Joe Davison, Sam Shleifer, Patrick von Platen, Clara Ma, Yacine Jernite, Julien Plu, Canwen Xu, Teven Le Scao, Sylvain Gugger, Mariama Drame, Quentin Lhoest, and Alexander M. Rush. Transformers: State-of-the-art natural language processing. In *Proceedings of the 2020 Conference on Empirical Methods in Natural Language Processing: System Demonstrations*, pages 38–45, Online, October 2020. Association for Computational Linguistics. URL <https://www.aclweb.org/anthology/2020.emnlp-demos.6>.
- Pengcheng Yin, Graham Neubig, Wen-tau Yih, and Sebastian Riedel. TaBERT: Pretraining for joint understanding of textual and tabular data. In *Proceedings of the 58th Annual Meeting of the Association for Computational Linguistics*, pages 8413–8426, Online, July 2020. Association for Computational Linguistics. doi: 10.18653/v1/2020.acl-main.745. URL <https://aclanthology.org/2020.acl-main.745>.

A Appendix

A.1 Constraint-aware training

As discussed in Section 4.4, to encourage GNN_2 to make structurally consistent predictions, we express a set of constraints on the complete labeling as follows. (1) A row and a column cannot both have compositions or constituents. (2) Composition and material ID must be orthogonally predicted (i.e., if a row has a composition, then the ID must be predicted in some column, and vice versa). (3) Constituents and material IDs must never be orthogonally predicted (that is, if rows have constituents, then another row in the table must have the ID). And, (4) material ID must occur at most once for the entire table. Let r_i and c_j be the predicted labels of row i and column j . Further let θ represent GNN_2 's parameters.

Constraint (1) is expressed as a hard constraint by:

$$r_i = l \Rightarrow c_j \neq l \quad \forall i \in \{1, \dots, R\}, j \in \{1, \dots, C\}, l \in \{1, 2\}.$$

Equivalent probabilistic statement is:

$$P(r_i = l; \theta) + P(c_j = l; \theta) - 1 \leq 0 \quad \forall i \in \{1, \dots, R\}, j \in \{1, \dots, C\}, l \in \{1, 2\}.$$

Constraint (2) can be written in the form of hard constraints as:

$$\begin{aligned} r_{i_1} = 1 &\Rightarrow r_{i_2} \neq 3 \quad \forall i_1, i_2 \in \{1, \dots, R\}, i_1 \neq i_2. \\ c_{j_1} = 1 &\Rightarrow c_{j_2} \neq 3 \quad \forall j_1, j_2 \in \{1, \dots, C\}, j_1 \neq j_2. \end{aligned}$$

Equivalent probabilistic statements are:

$$\begin{aligned} P(r_{i_1} = 1; \theta) + P(r_{i_2} = 3; \theta) - 1 &\leq 0 \quad \forall i_1, i_2 \in \{1, \dots, R\}, i_1 \neq i_2. \\ P(c_{j_1} = 1; \theta) + P(c_{j_2} = 3; \theta) - 1 &\leq 0 \quad \forall j_1, j_2 \in \{1, \dots, C\}, j_1 \neq j_2. \end{aligned}$$

We write constraint (3) in a hard constraint form as:

$$r_i = l \Rightarrow c_j \neq 5 - l \quad \forall i \in \{1, \dots, R\}, j \in \{1, \dots, C\}, l \in \{2, 3\}.$$

Equivalent probabilistic statement is:

$$P(r_i = l; \theta) + P(c_j = 5 - l; \theta) - 1 \leq 0 \quad \forall i \in \{1, \dots, R\}, j \in \{1, \dots, C\}, l \in \{2, 3\}.$$

Finally, hard versions of constraint (4) can be stated as:

$$\begin{aligned} r_{i_1} = 3 &\Rightarrow r_{i_2} \neq 3 \quad 1 \leq i_1 < i_2 \leq R. \\ c_{j_1} = 3 &\Rightarrow c_{j_2} \neq 3 \quad 1 \leq j_1 < j_2 \leq C. \\ r_i = 3 &\Rightarrow c_j \neq 3 \quad \forall i \in \{1, \dots, R\}, j \in \{1, \dots, C\}. \end{aligned}$$

Equivalent probabilistic statements are:

$$\begin{aligned} P(r_{i_1} = 3; \theta) + P(r_{i_2} = 3; \theta) - 1 &\leq 0 \quad 1 \leq i_1 < i_2 \leq R. \\ P(c_{j_1} = 3; \theta) + P(c_{j_2} = 3; \theta) - 1 &\leq 0 \quad 1 \leq j_1 < j_2 \leq C. \\ P(r_i = 3; \theta) + P(c_j = 3; \theta) - 1 &\leq 0 \quad \forall i \in \{1, \dots, R\}, j \in \{1, \dots, C\}. \end{aligned}$$

As explained in Section 4.4, we convert all these probabilistic statements to an auxiliary penalty term, which gets added in the loss function.

A.2 Dataset details

Table 4 presents some statistics about our dataset. Table 4a shows the number of tables in our dataset belonging to different table types. Further, Table 4b shows the total number of publications, materials, and tuples in all the three splits.

Table 4: Various statistics of our dataset for the three splits

Table Type	Splits		
	Train	Dev	Test
SCC	704	110	113
MCC-CI	626	132	132
MCC-PI	317	109	112
NC	2761	387	380
Total	4408	738	737

	Splits		
	Train	Dev	Test
Publications	1880	330	326
Materials	11207	2873	2649
Tuples	38799	10168	9514

A.3 Baseline models

In this section, we describe the details of our two baseline models: TAPAS and TAPAS-ADAPTED. Since, the TaPas Herzig et al. [2020] architecture has been used for QA over tables and we do not have any question in composition extraction task, we use table caption as a proxy for the question. We replace the empty table cells with special [EMPTY] token. The table caption and text in table cells are converted to wordpieces using the *LM* tokenizer. Then, we concatenate the wordpieces of caption and row-wise flattened table. Note that it is possible to obtain more than one wordpiece for some table cells. Since the input length after tokenization can be greater than 512, we truncate minimum possible rows from the end so that the length becomes less than or equal to 512. To avoid large number of rows getting truncated due to long caption, we truncate the caption so that it only contributes ≤ 100 wordpieces. To differentiate between the table cells belonging to different rows and/or columns, row and column index embeddings are added to the wordpiece embeddings in the TAPAS architecture. Position and Segment embeddings are same as in BERT Devlin et al. [2019], except that position indexes are incremented when table cell changes. Original TaPas architecture also involves adding different Rank embeddings to the input in order to answer rank based questions. We use the same rank embeddings for every table cell since there is no rank relation among the table cells for our case.

All these different type of embeddings are added together and passed through the *LM*. We take the contextual embedding of first word-piece of every table cell to be representative of it. Since we do not have row and column nodes here, row and column embeddings are computed by taking average of first wordpiece contextual embeddings of cells occurring in that row/column, which are then fed to a MLP for row/column classification. Edge embeddings are computed by concatenating the first wordpiece contextual embeddings of source and destination cells.

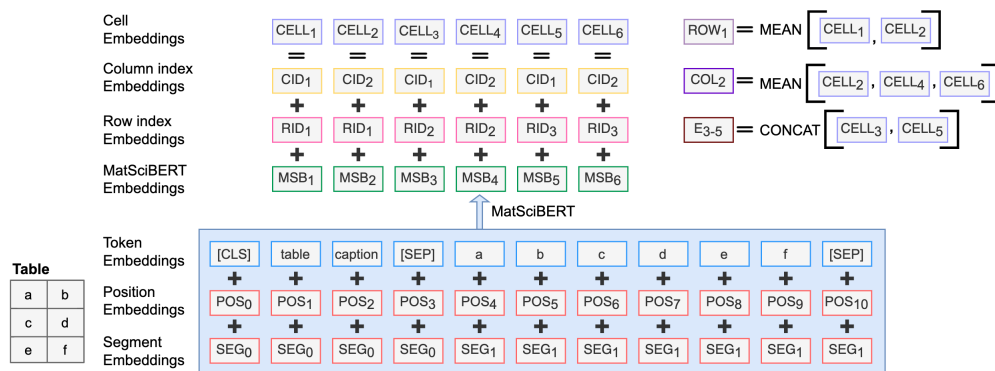


Figure 7: Schematic of TAPAS-ADAPTED baseline model

Figure 7 shows the schematic of TAPAS-ADAPTED model. Here, we initialize *LM* weights with that of MatSciBERT Gupta et al. [2022]. All other details are same as in the TAPAS model, except that here we add row and column index embeddings to MatSciBERT output, instead of input.

A.4 Hyper-parameter details

Now, we describe the hyper-parameters of DISCOMAT. Both GNN_1 and GNN_2 can have multiple hidden layers with different number of attention heads. We experiment with hidden layer sizes of 256, 128, and 64 and number of attention heads as 6, 4, and 2. We include residual connections in GAT, exponential linear unit (ELU) non-linearity after hidden layers, and LeakyRELU non-linearity (with slope $\alpha = 0.2$) to compute attention weights as done in Veličković et al. [2018]. Training is performed using 8 tables in a batch and we select the checkpoint with the maximum dev MatL F_1 score. We use a triangular learning rate and choose peak learning rate for LM to be among $1e-5$, $2e-5$, and $3e-5$ and peak learning rate for non- LM parameters to be among $3e-4$ and $1e-3$. Warmup ratio of 0.1 is used for all parameters. We further use batch normalization Ioffe and Szegedy [2015] and dropout Srivastava et al. [2014] probability of 0.2 in all MLPs. We use the same λ for every constraint penalty term. Embedding sizes for features are chosen from 128 and 256 and edge loss weight is selected among 0.3 and 1.0.

Table 5: Hyper-parameters for DISCOMAT

Hyper-parameter	GNN_1	GNN_2
GAT Hidden Layer Sizes	[256, 128, 64]	[128, 128, 64]
GAT Attention Heads	[4, 4, 4]	[6, 4, 4]
Peak LR for LM	$1e-5$	$2e-5$
Peak LR for non- LM	$3e-4$	$3e-4$
RegEx feature emb size	256	NA
Max-frequency feature emb size	256	128
Constraint penalty (λ)	50.0	30.0
Edge loss weight	NA	1.0

A.5 Corner cases

Figure 8 shows examples of some corner case tables. In Figure 8a, elements are being used as variables. Moreover, the values that variables can take are present in a single cell only. Figure 8b shows a table where units occur within the composition itself. Also, mixed units are being used to express the composition. Figure 8c comprises of compositions having both elements and compounds. Whereas, we made different REs for element compositions and different REs for compound compositions. Hence our REs are unable to match these.

(a)	(b)	(c)
<p>Glass composition (mol%)</p> <p>20Li₂O-20RO-60SiO₂ R = Mg, Ca, Sr, Ba</p> <p>xBaO-(100-x)B₂O₃ x = 20, 30, 40</p> <p>50RO-50P₂O₅ R = Ca, Sr, Ba</p> <p>xNa₂O-(30-x)CaO-60P₂O₅-10Al₂O₃ x = 0, 15, 30</p>	<p>Sample Composition</p> <p>1 0.6TeO₂-0.3TiO_{0.5}-0.1ZnO</p> <p>4 0.85TeO₂-0.15WO₃ + 0.1 wt%Ag₂O + 0.076 wt%CeO₂</p> <p>5 0.85TeO₂-0.15WO₃ + 0.1 wt% Ag₂O + 0.056 wt%CeO₂</p> <p>10 0.85TeO₂-0.15WO₃</p>	<p>0.91[Ge_{0.25}As_{0.1}Se_{0.65}]- 0.9[Ge_{0.25}As_{0.1}Se_{0.65}]-</p> <p>0.05GaS_{3/2}-0.04CsBr 0.05GaS_{3/2}-0.05CsBr</p> <p>τ_R 504 1170</p> <p>(μs)</p> <p>τ_m 98 937</p> <p>(μs)</p>

Figure 8: Examples of corner case composition tables (a) Murata et al. [2005] (b) Duclère et al. [2009] (c) Shin et al. [2002]

(a)	(b)	(c)																																																																
<table border="1"> <thead> <tr> <th>Sample code</th> <th>Composition</th> <th>Molar mass, M</th> <th>Density, d (g cm⁻³)</th> <th>Molar Volume, V_m (cm³ mol⁻¹)</th> </tr> <tr> <th></th> <th>M₂O₃ Al₂O₃ B₂O₃ TeO₂</th> <th>(g mol⁻¹)</th> <th>(g mol⁻¹)</th> <th>(cm³ mol⁻¹)</th> </tr> </thead> <tbody> <tr> <td>5W20BTe</td> <td>5 - 20 75</td> <td>145.216</td> <td>4.999 ± 0.001</td> <td>29.05</td> </tr> <tr> <td>5Nb20BTe</td> <td>5 - 20 75</td> <td>146.915</td> <td>4.877 ± 0.001</td> <td>30.12</td> </tr> <tr> <td>5Pb20BTe</td> <td>5 - 20 75</td> <td>144.785</td> <td>5.212 ± 0.001</td> <td>27.78</td> </tr> </tbody> </table>	Sample code	Composition	Molar mass, M	Density, d (g cm ⁻³)	Molar Volume, V _m (cm ³ mol ⁻¹)		M ₂ O ₃ Al ₂ O ₃ B ₂ O ₃ TeO ₂	(g mol ⁻¹)	(g mol ⁻¹)	(cm ³ mol ⁻¹)	5W20BTe	5 - 20 75	145.216	4.999 ± 0.001	29.05	5Nb20BTe	5 - 20 75	146.915	4.877 ± 0.001	30.12	5Pb20BTe	5 - 20 75	144.785	5.212 ± 0.001	27.78	<table border="1"> <thead> <tr> <th>Glass</th> <th>Na₂O</th> <th>Network modifiers</th> <th>Fe₂O₃ formers</th> <th>MnO</th> <th>SiO</th> <th>Other oxides</th> </tr> </thead> <tbody> <tr> <td>HLWMS-S (target)</td> <td>3.00</td> <td>CaO 0.00 Li₂O 6.00 K₂O 0.00</td> <td>Al₂O₃ 0.00 B₂O₃ 12.00 SiO₂ 33.50</td> <td>13.60</td> <td>29.90</td> <td>2.00</td> </tr> <tr> <td>HLWMS-11 (target)</td> <td>1.00</td> <td>CaO 0.00 Li₂O 3.50 K₂O 0.00</td> <td>Al₂O₃ 5.00 B₂O₃ 10.00 SiO₂ 30.00</td> <td>5.00</td> <td>13.60</td> <td>29.90</td> </tr> </tbody> </table>	Glass	Na ₂ O	Network modifiers	Fe ₂ O ₃ formers	MnO	SiO	Other oxides	HLWMS-S (target)	3.00	CaO 0.00 Li ₂ O 6.00 K ₂ O 0.00	Al ₂ O ₃ 0.00 B ₂ O ₃ 12.00 SiO ₂ 33.50	13.60	29.90	2.00	HLWMS-11 (target)	1.00	CaO 0.00 Li ₂ O 3.50 K ₂ O 0.00	Al ₂ O ₃ 5.00 B ₂ O ₃ 10.00 SiO ₂ 30.00	5.00	13.60	29.90	<table border="1"> <thead> <tr> <th>MnO</th> <th>Na₂O</th> <th>P₂O₅</th> </tr> <tr> <th>Nominal/analyzed</th> <th>Nominal/analyzed</th> <th>Nominal/analyzed</th> </tr> </thead> <tbody> <tr> <td>0/0</td> <td>50/46.7</td> <td>50/53.3</td> </tr> <tr> <td>5/4.6</td> <td>47.5/46.0</td> <td>47.5/49.6</td> </tr> <tr> <td>10/9.6</td> <td>45/43.2</td> <td>45/47.2</td> </tr> <tr> <td>15/14.7</td> <td>42.5/41.3</td> <td>42.5/44.1</td> </tr> </tbody> </table>	MnO	Na ₂ O	P ₂ O ₅	Nominal/analyzed	Nominal/analyzed	Nominal/analyzed	0/0	50/46.7	50/53.3	5/4.6	47.5/46.0	47.5/49.6	10/9.6	45/43.2	45/47.2	15/14.7	42.5/41.3	42.5/44.1
Sample code	Composition	Molar mass, M	Density, d (g cm ⁻³)	Molar Volume, V _m (cm ³ mol ⁻¹)																																																														
	M ₂ O ₃ Al ₂ O ₃ B ₂ O ₃ TeO ₂	(g mol ⁻¹)	(g mol ⁻¹)	(cm ³ mol ⁻¹)																																																														
5W20BTe	5 - 20 75	145.216	4.999 ± 0.001	29.05																																																														
5Nb20BTe	5 - 20 75	146.915	4.877 ± 0.001	30.12																																																														
5Pb20BTe	5 - 20 75	144.785	5.212 ± 0.001	27.78																																																														
Glass	Na ₂ O	Network modifiers	Fe ₂ O ₃ formers	MnO	SiO	Other oxides																																																												
HLWMS-S (target)	3.00	CaO 0.00 Li ₂ O 6.00 K ₂ O 0.00	Al ₂ O ₃ 0.00 B ₂ O ₃ 12.00 SiO ₂ 33.50	13.60	29.90	2.00																																																												
HLWMS-11 (target)	1.00	CaO 0.00 Li ₂ O 3.50 K ₂ O 0.00	Al ₂ O ₃ 5.00 B ₂ O ₃ 10.00 SiO ₂ 30.00	5.00	13.60	29.90																																																												
MnO	Na ₂ O	P ₂ O ₅																																																																
Nominal/analyzed	Nominal/analyzed	Nominal/analyzed																																																																
0/0	50/46.7	50/53.3																																																																
5/4.6	47.5/46.0	47.5/49.6																																																																
10/9.6	45/43.2	45/47.2																																																																
15/14.7	42.5/41.3	42.5/44.1																																																																

Figure 9: Some more examples of corner case composition tables (a) Kaur et al. [2015] (b) McKeown et al. [2003] (c) Omrani et al. [2014]

Figure 9 shows some more examples of corner cases. In Figure 9a, the first compound has to be inferred using the Material IDs. For example, W corresponds to WO₃ and Nb corresponds to Nb₂O₅. DISCOMAT makes the assumption that a composition is present in single row/column. Figure 9b

refutes this assumption as compositions are present in multiple rows. Sometimes researchers report both theoretical (nominal) and experimental (analyzed) compositions for the same material. Table in Figure 9c lists both type of compositions in the same cell and hence can't be extracted using DISCOMAT.